J. Fluid Mech. (2006), *vol.* 557, *pp.* 347–367.
doi:10.1017/S0022112006009888 Printed in the United Kingdom

The search for slow transients, and the effect of imperfect vertical alignment, in turbulent Rayleigh–Bénard convection

By GUENTER AHLERS, ERIC BROWN AND ALEXEI NIKOLAENKO

Department of Physics and iQUEST, University of California, Santa Barbara, CA 93106, USA

(Received 26 May 2005 and in revised form 17 November 2005)

We report experimental results for the influence of a tilt angle β relative to gravity on turbulent Rayleigh–Bénard convection of cylindrical samples. The measurements were made at Rayleigh numbers R up to 10^{11} with two samples of height L equal to the diameter D (aspect ratio $\Gamma \equiv D/L \simeq 1$), one with $L \simeq 0.5\,\mathrm{m}$ (the 'large' sample) and the other with $L \simeq 0.25\,\mathrm{m}$ (the 'medium' sample). The fluid was water with a Prandtl number $\sigma = 4.38$.

In contrast to the experiences reported by Chillà *et al.* (*Eur. Phys. J.* B, vol. 40, 2004, p. 223) for a similar sample but with $\Gamma \simeq 0.5$ ($D = 0.5$ and $L = 1.0\,\mathrm{m}$), we found no long relaxation times. For $R = 9.4 \times 10^{10}$ we measured the Nusselt number $\mathcal{N}$ as a function of β and obtained a small β dependence given by $\mathcal{N}(\beta) = \mathcal{N}_0[1-(3.1 \pm 0.1) \times 10^{-2}|\beta|]$ when β is in radians. This reduction of $\mathcal{N}$ is about a factor of 50 smaller than the result found by Chillà *et al.* (2004) for their $\Gamma \simeq 0.5$ sample.

We measured sidewall temperatures at eight equally spaced azimuthal locations on the horizontal mid-plane of the sample and used them to obtain cross-correlation functions between opposite azimuthal locations. The correlation functions had Gaussian peaks centred about $t_1^{cc} > 0$ that corresponded to half a turnover time of the large-scale circulation (LSC) and yielded Reynolds numbers Re^{cc} of the LSC. For the large sample and $R = 9.4 \times 10^{10}$ we found $Re^{cc}(\beta) = Re^{cc}(0) \times [1 + (1.85 \pm 0.21)|\beta| - (5.9 \pm 1.7)\beta^2]$. Similar results were obtained from the auto-correlation functions of individual thermometers. These results are consistent with measurements of the amplitude δ of the azimuthal sidewall temperature variation at the mid-plane that gave $\delta(\beta) = \delta(0) \times [1 + (1.84 \pm 0.45)|\beta| - (3.1 \pm 3.9)\beta^2]$ for the same R. An important conclusion is that the increase of the speed (i.e. of Re) of the LSC with β does not significantly influence the heat transport. Thus the heat transport must be determined primarily by the instability mechanism operative in the boundary layers, rather than by the rate at which 'plumes' are carried away by the LSC. This mechanism is apparently independent of β.

Over the range $10^9 \lesssim R \lesssim 10^{11}$ the enhancement of Re^{cc} at constant β due to the tilt could be described by a power law of R with an exponent of $-1/6$, consistent with a simple model that balances the additional buoyancy due to the tilt angle by the shear stress across the boundary layers. Even a small tilt angle dramatically suppressed the azimuthal meandering and the sudden reorientations characteristic of the LSC in a sample with $\beta = 0$. For large R the azimuthal mean of the temperature at the horizontal mid-plane differed significantly from the average of the top- and bottom-plate temperatures due to non-Boussinesq effects, but within our resolution was independent of β.

1. Introduction

Turbulent convection in a fluid heated from below, known as Rayleigh–Bénard convection (RBC), has been under intense study for some time (for reviews, see e.g. Siggia 1994; Kadanoff 2001; Ahlers, Grossmann & Lohse 2002). A central prediction of models for this system (Kraichnan 1962; Castaing *et al.* 1989; Shraiman & Siggia 1990; Grossmann & Lohse 2001) is the heat transported by the fluid. It is usually described in terms of the Nusselt number

$$\mathcal{N} = \frac{QL}{A\lambda\Delta T} \tag{1.1}$$

where Q is the heat current, L the cell height, A the cross-sectional area, λ the thermal conductivity, and ΔT the applied temperature difference. The Nusselt number depends on the Rayleigh number

$$R = \alpha g \Delta T L^3/\kappa\nu \tag{1.2}$$

and on the Prandtl number

$$\sigma = \nu/\kappa. \tag{1.3}$$

Here α is the isobaric thermal expansion coefficient, g the acceleration due to gravity, κ the thermal diffusivity, and ν the kinematic viscosity.

An important feature of turbulent RBC is the existence of a large-scale circulation (LSC) of the fluid (Krishnamurty & Howard 1981). For cylindrical samples of aspect ratio $\Gamma \equiv L/D \simeq 1$ the LSC is known to consist of a single cell, with fluid rising along the wall at some azimuthal location θ and descending along the wall at a location $\theta + \pi$ (see, for instance, Qiu & Tong 2001*a*; Sun *et al.* 2005*b*). As Γ decreases, the nature of the LSC is believed to change. For $\Gamma \lesssim 0.5$ it is expected (Verzicco & Camussi 2003; Stringano & Verzicco 2006; Sun *et al.* 2005*a*) that the LSC consists of two or more convection cells, situated vertically one above the other. Regardless of the LSC structure, the heat transport in turbulent RBC is mediated by the emission of hot (cold) volumes of fluid known as 'plumes' from a more or less quiescent boundary layer above (below) the bottom (top) plate. These plumes are swept away laterally by the LSC and rise (fall) primarily near the sidewall. Their buoyancy helps to sustain the LSC.

In a recent paper Chillà *et al.* (2004) reported measurements using a cylindrical sample of water with $\sigma \simeq 2.33$ and with $L = 1\,\mathrm{m}$ and $D = 0.5\,\mathrm{m}$ for $R \simeq 10^{12}$. Their sample thus had an aspect ratio $\Gamma \simeq 0.5$ near the boundary between a single-cell and a multi-cell LSC. They found exceptionally long relaxation times of $\mathcal{N}$ that they attributed to a switching of the LSC structure between two states. Multi-stability was also observed in Nusselt-number measurements by Roche *et al.* (2004) for a $\Gamma = 0.5$ sample (see also Nikolaenko *et al.* (2005) for a discussion of these data). Chillá *et al.* also found that $\mathcal{N}$ was reduced by tilting the sample through an angle β relative to gravity by an amount given approximately by $\mathcal{N}(\beta)/\mathcal{N}(0) \simeq 1 - 2\beta$ when β is measured in radians. A reduction by 2 % to 5 % of $\mathcal{N}$ (depending on R) due to a tilt by $\beta \simeq 0.035$ of a $\Gamma = 0.5$ sample was also reported recently by Sun *et al.* (2005*a*), although in that paper the β-dependence of this effect was not reported. Chillá *et al.* developed a simple model that yielded a reduction of $\mathcal{N}$ for the two-cell structure that was consistent in size with their measurements. Their model also assumes that no reduction of $\mathcal{N}$ should be found for a sample of aspect ratio near unity where the LSC is believed to consist of a single convection cell; they found some evidence to support this in the work of Belmonte, Tilgner & Libchaber (1995). Indeed, recent measurements by Nikolaenko *et al.* (2005) for $\Gamma = 1$ gave the same $\mathcal{N}$ within 0.1 % for a level sample and a sample tilted by 0.035 rad.

In this paper we report on a long-term study of RBC in a cylindrical sample with $\Gamma \simeq 1$. As expected, we found no long relaxation times because the LSC is uniquely defined. The establishment of a statistically stationary state after a large change of R occurred remarkably quickly, within a couple of hours, and thereafter there were no further long-term drifts over periods of many days.

We also studied the orientation θ_0 of the circulation plane of the LSC by measuring the sidewall temperature at eight azimuthal locations (Brown, Nikolaenko & Ahlers 2005*a*). With the sample carefully levelled (i.e. $\beta = 0$) we found θ_0 to change erratically, with large fluctuations. There were occasional relatively rapid reorientations, as observed before by Cioni, Ciliberto & Sommeria (1997) and by Sreenivasan, Bershadskii & Niemela (2002). The reorientations usually consisted of relatively rapid rotations, and rarely were reversals involving the cessation of the LSC followed by its re-establishment with a new orientation. This LSC dynamics yielded a broad probability distribution function $P(\theta_0)$, although a preferred orientation prevailed. When the sample was tilted relative to gravity through an angle β, a well-defined new orientation of the LSC circulation plane was established, $P(\theta_0)$ became much more narrow, and virtually all meandering and reorientation of the LSC was suppressed.

We found that $\mathcal{N}$ was reduced very slightly by tilting the sample. We obtained $\mathcal{N}(\beta) = \mathcal{N}_0[1 - (3.1 \pm 0.1) \times 10^{-2}|\beta|]$. This effect is about a factor of 50 smaller than the one observed by Chillá *et al.* for their $\Gamma = 0.5$ sample.

From sidewall-temperature measurements at two opposite locations we determined time cross-correlation functions $C_{i,j}$. The $C_{i,j}$ had a peak that could be fitted well by a Gaussian function, centred about a characteristic time t_1^{cc} that we interpreted as corresponding to the transit time needed by long-lived thermal disturbances to travel with the LSC from one side of the sample to the other, i.e. to half a turnover time of the LSC. We found that the β-dependence of the corresponding Reynolds number Re^{cc} is given by $Re^{cc}(\beta) = Re^{cc}(0) \times [1 + (1.85 \pm 0.21)|\beta| - (5.9 \pm 1.7)\beta^2]$. A similar result was obtained from the auto-correlation functions of individual thermometers. Thus there is an $O(1)$ effect of β on Re, and yet the effect of β on $\mathcal{N}$ was seen to be nearly two orders of magnitude smaller. We also determined the temperature amplitude δ of the azimuthal temperature variation at the mid-plane. We expect δ to be a monotonically increasing function of the speed of the LSC passing the mid-plane, i.e. of the Reynolds number. We found $\delta(\beta) = \delta(0) \times [1 + (1.84 \pm 0.45)|\beta| - (3.1 \pm 3.9)\beta^2]$. Thus, for small β its β-dependence is very similar to that of the Reynolds number.

From the large effect of β on Re and the very small effect on $\mathcal{N}$ we come to the important conclusion that the heat transport in this system is not influenced significantly by the strength of the LSC. This heat transport thus must be determined primarily by the efficiency of instability mechanisms in the boundary layers. It seems reasonable that these mechanisms should be nearly independent of β when β is small. This result is consistent with prior measurements by Ciliberto, Cioni & Laroche (1996), who studied the LSC and the Nusselt number in a sample with a rectangular cross-section. They inserted vertical grids above (below) the bottom (top) plate that suppressed the LSC, and found that within their resolution of 1 % or so the heat transport was unaltered. Their shadowgraph visualizations beautifully illustrate that the plumes are swept along laterally by the LSC when there are no grids and rise or fall vertically due to their buoyancy in the presence of the grids. Ciliberto *et al.* (1996) also studied the effect of tilting their rectangular sample by an angle of 0.17 rad. Consistent with the very small effect of tilting on $\mathcal{N}$ found by us, they found that within their resolution the heat transport remained unaltered.

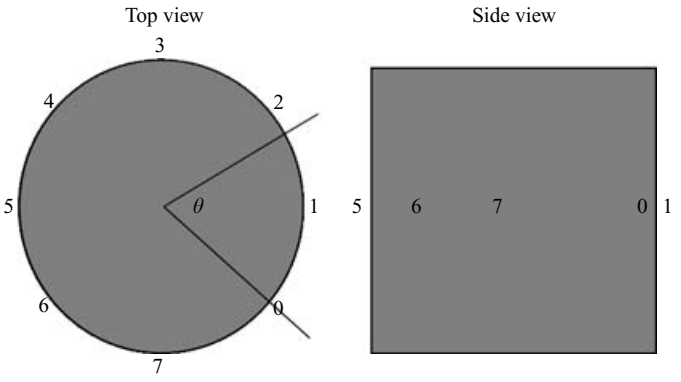

FIGURE 1. A schematic diagram of the sample, showing the location of the eight sidewall thermometers.

We observed that the sudden reorientations of the LSC that are characteristic of the level sample are strongly suppressed by even a small tilt angle.

2. Apparatus and data analysis

For the present work we used the 'large' and the 'medium' sample and apparatus described in detail by Brown *et al.* (2005*b*). Copper top and bottom plates each contained five thermistors close to the copper–fluid interface. The bottom plate had imbedded in it a resistive heater capable of delivering up to 1.5 kW uniformly distributed over the plate. The top plate was cooled via temperature-controlled water circulating in a double-spiral channel. For the Nusselt-number measurements a temperature set point for a digital feedback regulator was specified. The regulator read one of the bottom-plate thermometers at time intervals of a few seconds and provided appropriate power to the heater. The top-plate temperature was determined by the temperature-controlled cooling water from two Neslab RTE740 refrigerated circulators.

Each apparatus was mounted on a base plate that in turn was supported by three legs consisting of long threaded rods passing vertically through the plate. The entire apparatus thus could be tilted by an angle β relative to the gravitational acceleration by turning one of the rods. The maximum tilt angle attainable was 0.12 (0.21) rad for the large (medium) sample. For positive β the tilt was oriented so that the easterly part of the cell became elevated. At the beginning of each run at a given tilt angle we waited for several hours before taking data. A given run would then last from about one to several days.

The Nusselt number was calculated using the temperatures recorded in each plate and the power dissipated in the bottom-plate heater. The sidewall was Plexiglas of thickness 0.64 cm (0.32 cm) for the large (medium) sample. It determined the length L of the sample. Around a circumference the height was uniformly 50.62 ± 0.01 cm (24.76 ± 0.01 cm) for the large (medium) sample. The inside diameter was $D = 49.70 \pm 0.01$ cm ($D = 24.84 \pm 0.01$ cm) for the large (medium) sample. The end plates had anvils that protruded into the sidewall, thus guaranteeing a circular cross-section near the ends. For the large sample we made measurements of the outside diameter near the half-height after many months of measurements and found that this diameter varied around the circumference by less than 0.1 %.

Imbedded in the sidewall and within 0.06 cm of the fluid–Plexiglas interface were eight thermistors, equally spaced azimuthally and positioned vertically at half the height of the sample. Their location is illustrated in figure 1. Figure 2 shows a typical

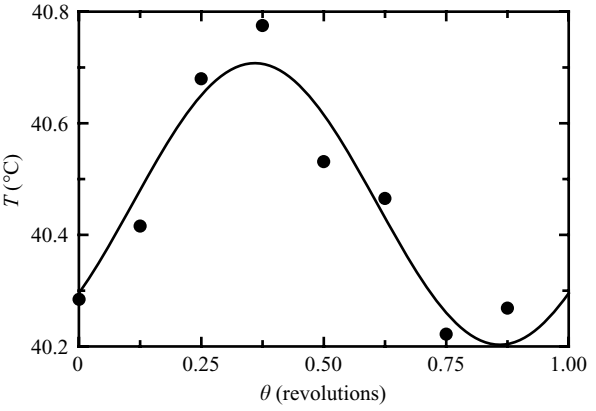

FIGURE 2. A example of the sidewall temperature at the horizontal mid-plane for the medium sample as a function of the azimuthal angle θ at $R = 1.1 \times 10^{10}$. The solid line is a fit of (2.1) to the data.

example of their temperatures as a function of azimuthal position. We interpret the relatively high (low) temperature readings as the angular positions where there was up-flow (down-flow) of the LSC. A fit of

$$T_i = T_c + \delta \cos(i\pi/4 - \theta_0), \;\; i = 0, \ldots, 7, \tag{2.1}$$

is shown as the solid line in the figure and yielded the mean centre temperature T_c, the angular orientation θ_0 of the LSC (relative to the location of thermistor 0), and a measure δ of the LSC strength. The seemingly random scatter of the data about the fitted function reflects the turbulent nature of the flow; the thermometer resolution was of order 10^{-3} °C.

We do not have a quantitative model for the dependence of δ on R and Re, but expect the size of δ to be influenced by the heat transport across a viscous boundary layer separating the LSC from the sidewall. Thus δ should increase with Rayleigh number because the azimuthal temperature variation carried by the LSC near the boundary layer increases with R. At constant R we expect δ to increase with the LSC Reynolds number Re because the boundary-layer thickness is expected to decrease with Re as $1/Re^{1/2}$. Experimentally we find, over the range $5 \times 10^9 < R < 10^{11}$ and for the large sample, that δ is related to R by an effective power law $\delta \propto R^{0.81}$, whereas $Re \propto R^{0.50}$ in this range.

From time series of the $T_i(t)$ taken at intervals of a few seconds and covering at least one day we determined the cross-correlation functions $C^{i,j}(\tau)$ corresponding to signals at azimuthal positions displaced around the circle by π (i.e. $j = i + 4$). These functions are given by

$$C^{i,j}(\tau) = \langle [T_i(t) - \langle T_i(t) \rangle_t] \times [T_j(t+\tau) - \langle T_j(t) \rangle_t] \rangle_t. \tag{2.2}$$

We also calculated the auto-correlation functions corresponding to $i = j$ in (2.2), for all eight thermometers.

Initially each sample was carefully levelled so that the tilt angle relative to gravity was less than 10^{-3} rad. Later it was tilted deliberately to study the influence of a non-zero β on the heat transport.

The fluid was water at 40 °C where $\alpha = 3.88 \times 10^{-4}$ K^{-1}, $\kappa = 1.53 \times 10^{-3}$ cm^2 s^{-1}, and $\nu = 6.69 \times 10^{-3}$ cm^2 s^{-1}, yielding $\sigma = 4.38$.

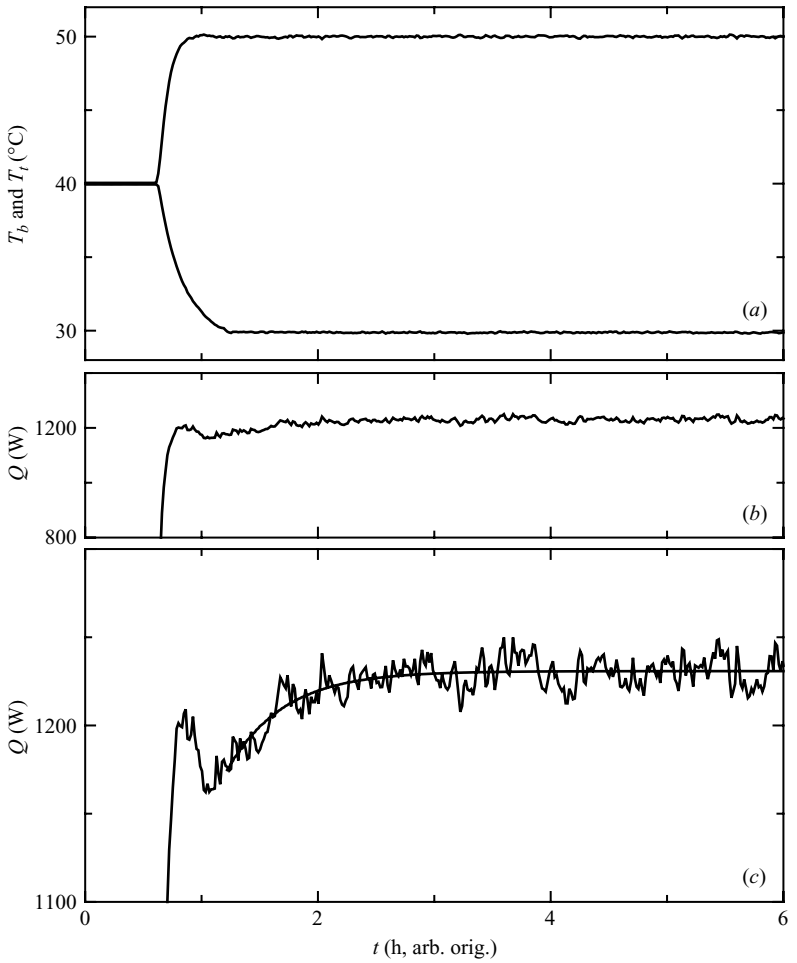

FIGURE 3. Time evolution of the top- and bottom-plate temperatures and of the heat current for the large sample. Initially the temperature difference was $\Delta T \simeq 0$. At $t = 0.6$ h the top- and bottom-plate regulators were given new set points corresponding to $\Delta T = 20\,^{\circ}\mathrm{C}$ ($R = 9.43 \times 10^{10}$). (*a*) Top- (lower data set, T_t) and bottom- (upper data set, T_b) plate temperatures. (*b*) Heat current Q delivered by the temperature regulator designed to hold T_b at a specified value. (*c*) Heat current Q on an expanded scale. The solid line represents a fit of an exponential function to the data for $t > 1.2$ h that gave a relaxation time $\tau_Q = 0.48$ h.

3. The Nusselt number of a vertical sample

3.1. *Initial transients*

In figure 3(*a*) we show the initial evolution of the top and bottom temperatures of the large sample in a typical experiment. Initially the heat current was near zero and T_b and T_t were close to 40 °C. The sample had been equilibrated under these conditions for over one day. Near $t = 0.6$ h a new temperature set point of 50 °C was specified for the bottom plate, and the circulator for the top plate was set to provide $T_t \simeq 30\,^{\circ}\mathrm{C}$. Figure 3(*a*) shows that there were transients that lasted until about 0.9 h (1.2 h) for T_b (T_t). These transients are determined by the response time and power capability of the bottom-plate heater and the top-plate cooling water and are unrelated to hydrodynamic phenomena in the liquid. Figures 3(*b*) and 3(*c*) show the

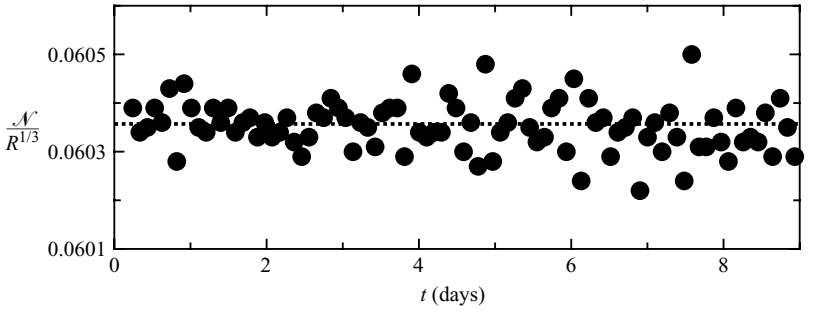

FIGURE 4. The reduced Nusselt number $\mathcal{N}/R^{1/3}$ for $R = 9.43 \times 10^{10}$ for the large sample as a function of time during a single experimental run that lasted 9 days. Each data point is based on temperature and heat-current averages over a time interval of 2 h. The dotted line corresponds to the value estimated by using all the data. Note that the entire vertical axis covers only a change of 0.8 %. The mean value is 0.06035, and the standard deviation from the mean is 5.1×10^{-5} or 0.084 %.

evolution of the heat current. After the initial rapid rise until $t \simeq 0.8$ h the current slowly evolved further to a statistically stationary value until $t \simeq 3$ h. A fit of the exponential function $Q(t) = Q_\infty - \Delta Q \exp(-t/\tau_Q)$ to the data for $t > 1.2$ h is shown by the solid line in figure 3(*c*) and yielded a relaxation time $\tau_Q = 0.48 \pm 0.04$ h. We attribute this transient to the evolution of the fluid flow. Indeed, τ_Q is similar in size to the length of transients found by Xi, Lam & Xia (2004) from shadowgraph images of plumes. It is interesting to compare τ_Q with intrinsic time scales of the system. The vertical thermal diffusion time $\tau_v \equiv L^2/\kappa$ is 467 h. Obviously it does not control the establishment of the stationary state. If we assume that it may be reduced by a factor of $1/\mathcal{N}$ with $\mathcal{N} = 263$, we still obtain a time sale of 1.78 h that is longer than τ_Q. We believe that the relatively rapid equilibration is associated with the establishment of the top and bottom boundary layers that involve much shorter lengths l_t and l_b. It also is necessary for the LSC to establish itself; but, as we shall see, its precise Reynolds number is unimportant for the heat transport. In addition, the LSC can be created relatively fast since this is not a diffusive process.

3.2. *Results under statistically stationary conditions*

Figure 3 shows the behaviour of the system only during the first six hours and does not exclude the slow transients reported by Chillà *et al.* that occurred over time periods of $O(10^2)$ h. Thus we show in figure 4 results for $\mathcal{N}/R^{1/3}$ from a run using the large sample that was continued under constant externally imposed conditions for 9 days. Each point corresponds to a value of $\mathcal{N}$ based on a time average over 2 h of the plate temperatures and the heat current. Note that the vertical range of the entire graph is only 0.8 %. Thus, within a small fraction of 1 %, the results are time independent. Indeed, during nearly a year of data acquisition for a $\Gamma = 1$ sample at various Rayleigh numbers, involving individual runs lasting from one to many days, we have never found long-term drifts or changes of $\mathcal{N}$ after the first few hours. This differs dramatically from the observations of Chillà *et al.* who found changes by about 2 % over about 4 days for their $\Gamma = 0.5$ sample.

One might ask whether our runs of up to nine days were long enough to detect the slow transients reported by Chillà *et al.*, if they are present in our $\Gamma = 1$ system. Chillà *et al.* suggested that the time scale required to find the transients is comparable to the 'diffusion time of the whole cell'. We note that our sample, with $L \simeq 0.5$ m, has only half the height of the $\Gamma = 0.5$ sample of Chillà *et al.* ($L = 1$ m) and thus only

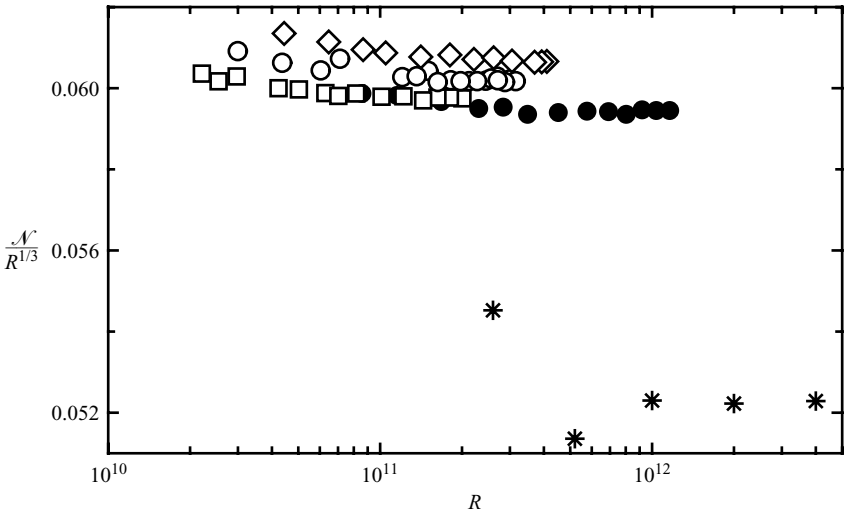

FIGURE 5. The reduced Nusselt number $\mathcal{N}/R^{1/3}$ as a function of the Rayleigh number R. Stars: data from Chillà *et al.* (2004) for $\sigma = 2.3$ and $\Gamma = 0.5$. Solid circles: data from Nikolaenko *et al.* (2005) for $\sigma = 4.38$ and $\Gamma = 0.43$. Open symbols: from Nikolaenko *et al.* (2005) for $\Gamma = 0.67$, with open squares: $\sigma = 5.42$; open circles: $\sigma = 4.38$; open diamonds: $\sigma = 3.62$.

one quarter the diffusion time. Thus our run duration of nine days, when scaled by this time, is comparable to the run time of over a month used by Chillà *et al.*

To document further the stationary nature of the system, we have compared results from the large sample for $\mathcal{N}$ obtained from many runs, each of one to ten days' duration, over a period of about five months (Nikolaenko *et al.* 2005; Funfschilling *et al.* 2005). The scatter of the data at a given R is only about 0.1 %. This excellent reproducibility would not be expected if there were slow transients due to transitions between different states of the LSC.

Although work in our laboratory with other aspect ratios has been less extensive, we also have not seen any evidence of drifts or transients for the larger $\Gamma = 1.5, 2, 3,$ and 6 (Funfschilling *et al.* 2005; Brown *et al.* 2005*b*) nor for the smaller $\Gamma = 0.67, 0.43,$ and 0.28 (Nikolaenko *et al.* 2005; Brown *et al.* 2005*b*). It may be that $\Gamma = 0.5$, being near the boundary between a single-cell LSC and more complicated LSC structures (Verzicco & Camussi 2003; Stringano & Verzicco 2006; Sun *et al.* 2005*a*), is unique in this respect.

In figure 5 we compare results for $\mathcal{N}/R^{1/3}$ from our large sample (Nikolaenko *et al.* 2005) with those reported by Chillà *et al.* (stars). Our results are larger by about 15 %. To find a reason for this difference, we first look at the Γ and σ dependence. The open (solid) circles represent our data for $\sigma = 4.38$ and $\Gamma = 0.67$ (0.43) and show that the dependence of $\mathcal{N}$ on Γ is not very strong. The open squares (diamonds) are our results for $\Gamma = 0.67$ and $\sigma = 5.42$ (3.62) and indicate that $\mathcal{N}$ actually increases slightly with σ. Thus the lower values of $\mathcal{N}$ (compared to ours) obtained by Chillá *et al.* for $\sigma = 2.3$ and $\Gamma = 0.5$ cannot be explained in terms of the Γ and σ dependence of $\mathcal{N}$. Some of the difference can be attributed to non-Boussinesq effects that tend to reduce $\mathcal{N}$ (Funfschilling *et al.* 2005). However, for the largest ΔT used by Chillá *et al.* (31 °C) we expect this effect to be somewhat less than 1 % (Funfschilling *et al.* 2005; Ahlers *et al.* 2006). Finally, the effect of the finite conductivity of the top and bottom plates should be considered. This can reduce $\mathcal{N}$ by several percent when ΔT

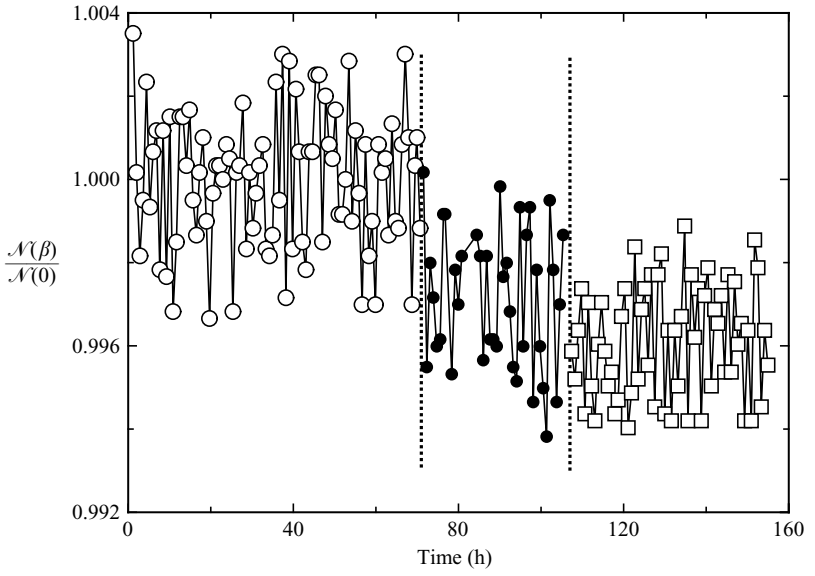

FIGURE 6. The reduced Nusselt number $\mathcal{N}(\beta)/\mathcal{N}(0)$ as a function of time for the large sample and $R = 9.43 \times 10^{10}$. Open circles: tilt angle $\beta = 0$. Solid circles: $\beta = 0.087$ rad. Open squares: $\beta = 0.122$ rad. All data are normalized by the average $\mathcal{N}(0)$ of the data for $\beta = 0$. Each data point is based on temperature and heat-current measurements over a 2 h period. The vertical dotted lines indicate the times when β was changed.

is large (Chaumat, Castaing & Chillà 2002; Verzicco 2004; Brown *et al.* 2005*b*), but it is difficult to say precisely by how much. It seems unlikely that this effect can explain the entire difference, particularly at the smaller R (and thus ΔT) where it is relatively small.

4. Tilt-angle dependence of the Nusselt number

In figure 6 we show results for $\mathcal{N}$ from the large sample at $R = 9.43 \times 10^{10}$. Each data point was obtained from a 2 h average of measurements of the various temperatures and of Q. Three data sets, taken in temporal succession, for tilt angles $\beta = 0$, 0.087, and 0.122 rad are shown. All data were normalized by the mean of the results for $\beta = 0$. Typically, the standard deviation from the mean of the data at a given β was 0.13 %. The vertical dotted lines and the change in the data symbols show where β was changed. Tilting the cell caused a small but measurable reduction on $\mathcal{N}$. In figure 7 we show the mean value for each tilt angle, obtained from runs of at least a day's duration at each β, as a function of $|\beta|$. $\mathcal{N}$ decreases linearly with β. A fit of a straight line to the data yielded

$$\mathcal{N}(\beta) = \mathcal{N}_0[1 - (3.1 \pm 0.1) \times 10^{-2}|\beta|], \tag{4.1}$$

with $\mathcal{N}_0 = 273.5$. Simlar results for the medium cell are compared with the large-cell results in figure 8. At the smaller Rayleigh number of the medium sample the effect of β on $\mathcal{N}$ is somewhat less. Because the effect of β on $\mathcal{N}$ is so small, we did not make a more detailed investigation of its Rayleigh-number dependence.

Chillà *et al.* proposed a model that predicts a significant tilt-angle effect on $\mathcal{N}$ for $\Gamma = 0.5$ where they assume the existence of two LSC cells, one above the other. They also assumed that there would be no effect for $\Gamma = 1$ where there is only one LSC

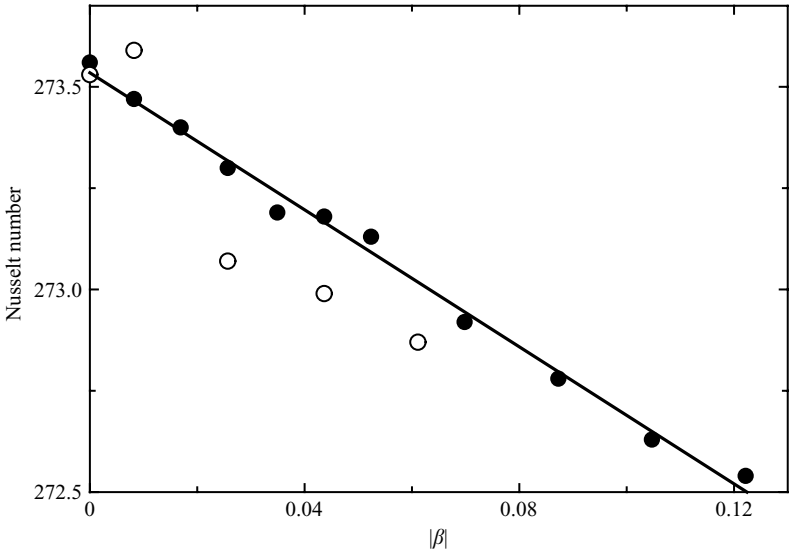

FIGURE 7. The Nusselt number $\mathcal{N}(\beta)$ as a function of the tilt angle β for the large sample with $R = 9.43 \times 10^{10}$. Each point is the average over an entire run of duration one day or longer. Solid circles: $\beta > 0$. Open circles: $\beta < 0$. The solid line is a least-squares fit of a straight line (4.1) to the data for $\beta > 0$.

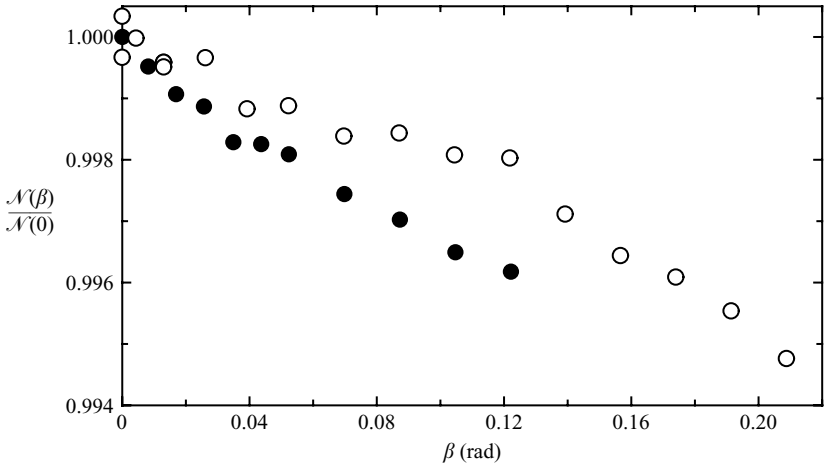

FIGURE 8. The reduced Nusselt number $\mathcal{N}(\beta)/\mathcal{N}_0$ as a function of the tilt angle β for the large sample with $R = 9.43 \times 10^{10}$ (solid circles) and the medium sample with $R = 1.13 \times 10^{10}$ (open circles).

cell. Although we found an effect for our $\Gamma = 1$ sample, we note that it is a factor of about 50 smaller than the effect observed by Chillà *et al.* for $\Gamma = 0.5$.

5. Tilt-angle dependence of the large-scale circulation

5.1. *The orientation*

In figure 9 we show the angular orientation θ_0 (*a*) and the temperature amplitude δ (*b*) of the LSC. For the first 8000 s shown in the figure, the sample was level ($\beta = 0.000 \pm 0.001$). θ_0 varied irregularly with time. The probability distribution

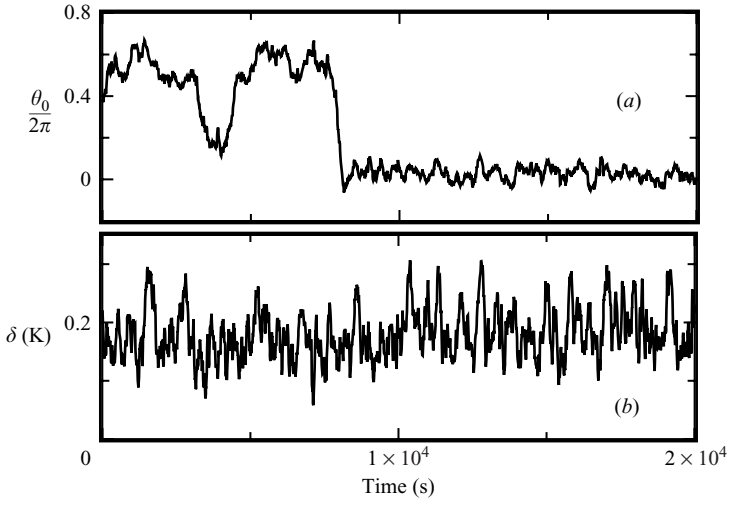

FIGURE 9. (*a*) The orientation θ_0 of the plane of circulation and (*b*) the temperature amplitude δ of the large-scale circulation as a function of time for the large sample and $R = 9.43 \times 10^{10}$. At $t = 8000$ s the sample was tilted by an angle $\beta = 0.087$ rad relative to gravity.

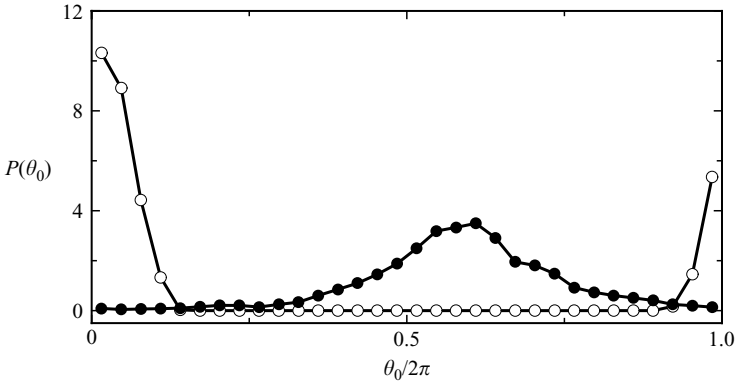

FIGURE 10. The probability distribution $P(\theta_0)$ of the orientation θ_0 of the plane of circulation of the large-scale flow for the large sample and $R = 9.43 \times 10^{10}$ as a function of θ_0. Solid circles: tilt angle $\beta = 0 \pm 0.001$. Open circles: $\beta = 0.087$ rad.

function $P(\theta_0)$ is shown in figure 10 as solid dots. Essentially all angles are sampled by the flow, but there is a preferred direction close to $\theta_0/2\pi = 0.6$. At $t = 8000$ s, the sample was tilted through an angle $\beta = 0.087$ rad. The direction of the tilt was chosen deliberately so as to oppose the previously prevailing preferred orientation. As a consequence there is a sharp transition with a change of θ_0 by approximately π. The temperature amplitude δ on average increased slightly, and certainly remained non-zero. From this we conclude that the transition took place via rotation of the LSC, and not by cessation that would have involved a reduction of δ to zero (see Brown *et al.* 2005*a*). We note that $\theta_0(t)$ fluctuated much less after the tilt. The results for $P(\theta_0)$ after the tilt are shown in figure 10 as open circles. They confirm that the maximum was shifted close to $\theta_0 = 0$, and that the distribution was much more narrow.

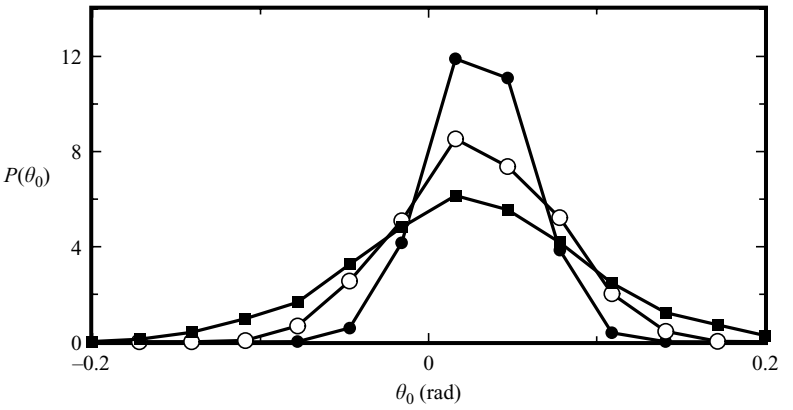

FIGURE 11. The probability distribution $P(\theta_0)$ of the orientation θ_0 of the plane of circulation of the large-scale flow for the large sample and $R = 9.43 \times 10^{10}$ at three tilt angles β. Solid circles: $\beta = 0.122$ rad. Open circles: $\beta = 0.044$ rad. Solid squares: $\beta = 0.026$ rad.

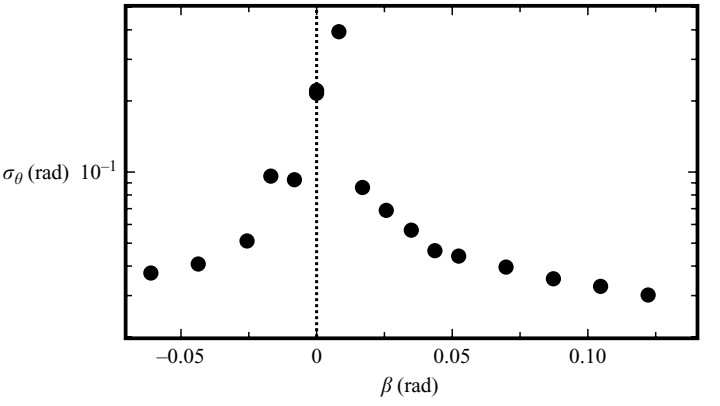

FIGURE 12. The square root of the variance σ_θ of the probability distribution $P(\theta_0)$ of the orientation θ_0 of the plane of circulation of the large-scale flow for the large sample and $R = 9.43 \times 10^{10}$ as a function of the tilt angle β.

In figure 11 we show $P(\theta_0)$ for $\beta = 0.122$ (solid circles), 0.044 (open circles), and 0.026 (solid squares). A reduction of β leads to a broadening of $P(\theta_0)$. The square root of the variance of data like those in figure 11 is shown in figure 12 on a logarithmic scale as a function of β on a linear scale. Even a rather small tilt angle caused severe narrowing of $P(\theta_0)$.

5.2. *The temperature amplitude*

In figure 13 we show the temperature amplitude $\delta(\beta)$ of the LSC as a function of β. As was the case for $\mathcal{N}$, the data are averages over the duration of a run at a given β (typically a day or two). The solid (open) circles are for positive (negative) β. The data can be represented well by either a linear or a quadratic equation. A least-squares fit yielded

$$\delta(\beta) = \delta(0) \times [1 + (1.84 \pm 0.45)|\beta| - (3.1 \pm 3.9)\beta^2] \tag{5.1}$$

with $\delta(0) = 0.164$ K.

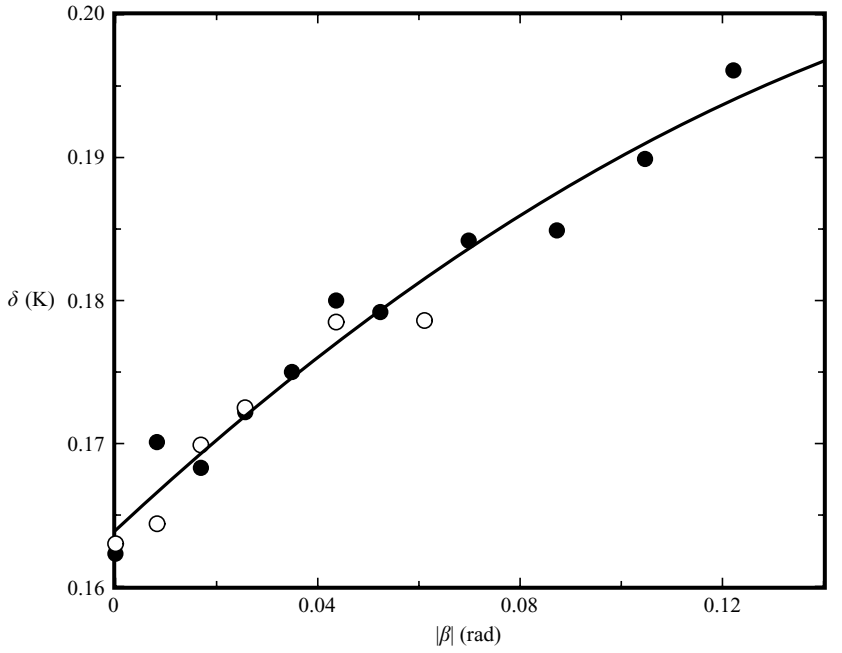

FIGURE 13. The time-averaged temperature amplitude $\delta(\beta)$ of the LSC for the large sample as a function of $|\beta|$. Solid circles: $\beta \geqslant 0$. Open circles: $\beta < 0$. For this example $R = 9.43 \times 10^{10}$.

5.3. *The Reynolds numbers*

Using (2.2), we calculated the auto-correlation functions (AC) $C^{i,i}$, $i = 0, \ldots, 7$, as well as the cross-correlation functions (CC) $C^{i,j}$, $j = [(i + 4) \bmod 8]$, $i = 0, \ldots, 7$, of the temperatures measured on opposite sides of the sample. Typical examples are shown in figure 14. The CC has a characteristic peak that we associate with the passage of relatively hot or cold volumes of fluid at the thermometer locations. Such temperature cross-correlations have been shown, e.g. by Qiu & Tong (2001*b*, 2002), to yield delay times equal to those of velocity-correlation measurements, indicating that warm or cold fluid volumes travel with the LSC. The function

$$C^{i,j}(\tau) = -b_0 \exp\left(-\frac{\tau}{\tau_0^{i,j}}\right) - b_1 \exp\left[-\left(\frac{\tau - t_1^{i,j}}{\tau_1^{i,j}}\right)^2\right], \tag{5.2}$$

consisting of an exponentially decaying background (that we associate with the random time evolution of θ_0) and a Gaussian peak, was fitted to the data for the CC. The fitted function is shown in figure 14 as a solid line over the range of τ used in the fit. It is an excellent representation of the data and yields the half turnover time $\mathscr{T}/2 = t_1^{i,j}$ of the LSC. Similarly, we fitted the function

$$C^{i,i}(\tau) = b_0 \exp\left(-\frac{\tau}{\tau_0^{i,i}}\right) + b_1 \exp\left[-\left(\frac{\tau}{\tau_1^{i,i}}\right)^2\right] + b_2 \exp\left[-\left(\frac{\tau - t_2^{i,i}}{\tau_2^{i,i}}\right)^2\right] \tag{5.3}$$

to the AC data. It consists of two Gaussian peaks, one centred at $\tau = 0$ and the other at $\tau = t_2^{i,i}$, and the exponential background. We interpret the location $t_2^{i,i}$ of the second Gaussian peak as corresponding to a complete turnover time $\mathscr{T}$ of the LSC.

In terms of the averages $\langle t_1^{i,j} \rangle$ and $\langle t_2^{i,i} \rangle$ over all 8 thermometers or thermometer-pair combinations we define (Qiu & Tong 2002; Grossmann & Lohse 2002) the Reynolds

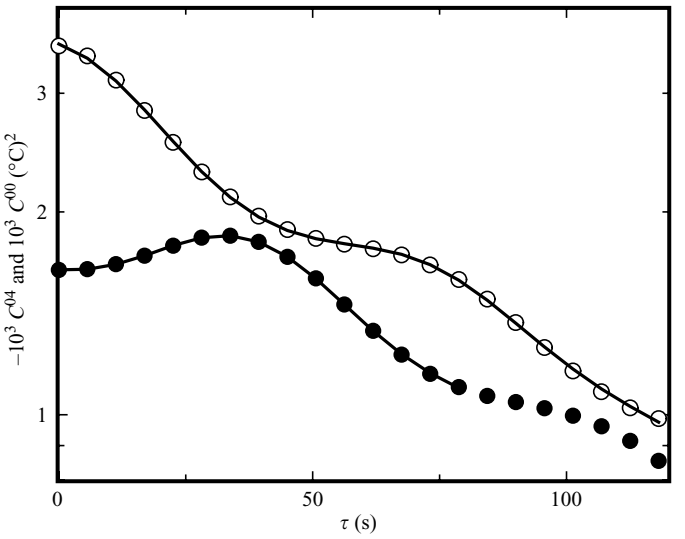

FIGURE 14. The cross-correlation function $C^{04}(\tau)$ between thermometers 0 and 4 (solid circles) and the auto-correlation function $C^{00}(\tau)$ of thermometer 0 (open circles) for the large sample. The solid lines are fits of (5.2) and (5.3) to the data. They also indicate the range of τ used for the fits. For this example the tilt angle was $\beta = -0.009$ and $R = 9.43 \times 10^{10}$.

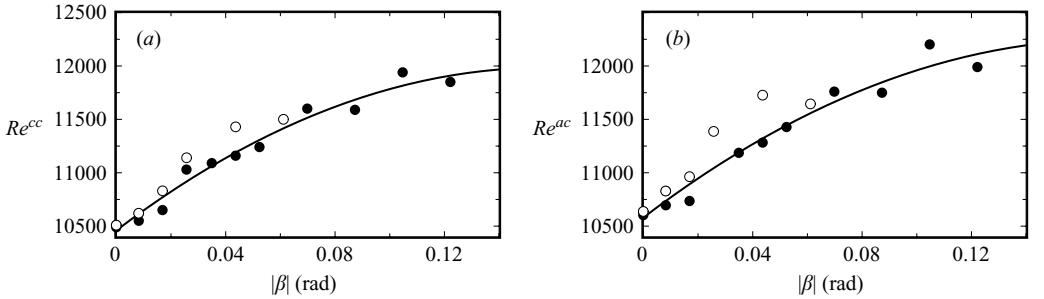

FIGURE 15. (*a*) The Reynolds number $Re^{cc}(|\beta|)$ obtained from the temperature cross-correlation functions, and (*b*) the Reynolds number $Re^{ac}(|\beta|)$ obtained from the temperature auto-correlation functions, of the LSC for the large sample and $R = 9.43 \times 10^{10}$ as a function of the absolute value $|\beta|$ of the tilt angle. Solid circles: $\beta \geqslant 0$. Open circles: $\beta < 0$. The Rayleigh number was 9.43×10^{10}.

numbers

$$Re^{cc} = \left(L/\left\langle t_1^{i,j}\right\rangle\right)(L/\nu) \tag{5.4}$$

and

$$Re^{ac} = \left(2L/\left\langle t_2^{i,i}\right\rangle\right)(L/\nu). \tag{5.5}$$

Here the length scale $2L$ was used to convert the turnover time $\mathscr{T}$ into an LSC speed $2L/\mathscr{T}$. For $\Gamma = 1$, the length $4L$ might have been used instead, as was done for instance by Lam, Shang & Xia (2002). This would have led to a Reynolds number larger by a factor of two. In figure 15(*a*) and 15(*b*) we show $Re^{cc}(|\beta|)$ and $Re^{ac}(|\beta|)$ respectively. The solid circles are for positive and the open ones for negative β. Initially $Re^{cc}(|\beta|)$ and $Re^{ac}(|\beta|)$ grow linearly with β, but the data also reveal some curvature as $|\beta|$ becomes larger. Thus we fitted quadratic equations to the data and

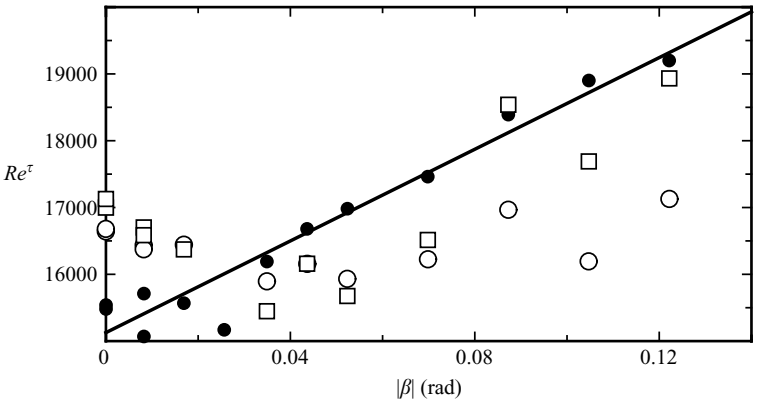

FIGURE 16. The Reynolds number $Re^\tau(|\beta|)$ obtained from the half-widths τ_1 of the temperature cross-correlation functions (solid circles) and from the half-widths τ_1 (open squares) and τ_2 (open circles) of the temperature auto-correlation functions as a function of the tilt angle. The Rayleigh number was 9.43×10^{10}.

obtained

$$Re^{cc}(\beta) = Re^{cc}(0) \times [1 + (1.85 \pm 0.21)|\beta| - (5.9 \pm 1.7)\beta^2] \tag{5.6}$$

and

$$Re^{ac}(\beta) = Re^{ac}(0) \times [1 + (1.72 \pm 0.38)|\beta| - (4.1 \pm 3.2)\beta^2] \tag{5.7}$$

with $Re^{cc}(0) = 10467 \pm 43$ and $Re^{ac}(0) = 10565 \pm 82$ (all parameter errors are 67 % confidence limits). The results for $Re^{cc}(0)$ and $Re^{ac}(0)$ are about 10 % higher than the prediction by Grossmann & Lohse (2002) for our σ and R. The excellent agreement between Re^{cc} and Re^{ac} is consistent with the idea that the CC yields $\mathscr{T}/2$ and that the AC gives $\mathscr{T}$. As expected (see § 2), the β-dependences of both Reynolds numbers are the same within their uncertainties. It is interesting to see that the coefficients of the linear term also agree with the corresponding coefficient for δ (equation (5.1)). This suggests that there may be a closer relationship between δ and Re than we would have expected *a priori*. However, the coefficient of the linear term in (5.6) or (5.7) is larger by a factor of about 50 than the corresponding coefficient for the Nusselt number in (4.1).

Although the precise meaning of the half-widths τ_1 and τ_2 in (5.2) and (5.3) is less clear than that of t_1 and t_2, it is of some interest to compute the corresponding Reynolds numbers Re^τ from (5.4). These are shown in figure 16. They are about 40 % larger than Re^{ac} or Re^{cc}, and all three are of about the same size. The results obtained from the AC show considerable scatter, and the β-dependence is not resolved very well. On the other hand, the result from the half-width of the Gaussian peak of the CC is more precise, and a fit of a straight line to the data yields $Re^\tau = Re^\tau(0) \times (1 + 2.27|\beta|)$ with $Re^\tau(0) = 15130$.

In figure 17 we show measurements of Re^{cc} and of δ, each normalized by its value at $\beta = 0$, as a function of β for the medium sample and $R = 1.13 \times 10^{10}$. For this sample we were able to attain larger values of β than for the large one. It is seen that δ and Re^{cc} have about the same β dependence for small β, but that δ then increases more rapidly than Re^{cc} as β becomes large. Although we do not know the reason for this behaviour, it suggests that the larger speed of the LSC enhances the thermal contact between the sidewall and the fluid interior.

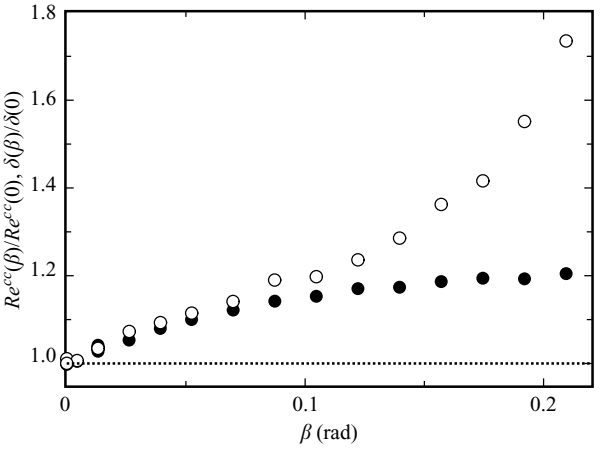

FIGURE 17. The Reynolds-number ratio $Re^{cc}(\beta)/Re^{cc}(0)$ (solid circles) obtained from the temperature cross-correlation functions, and the amplitude ratio $\delta(\beta)/\delta(0)$ (open circles), of the LSC of the medium sample for $R = 1.13 \times 10^{10}$ as a function of β.

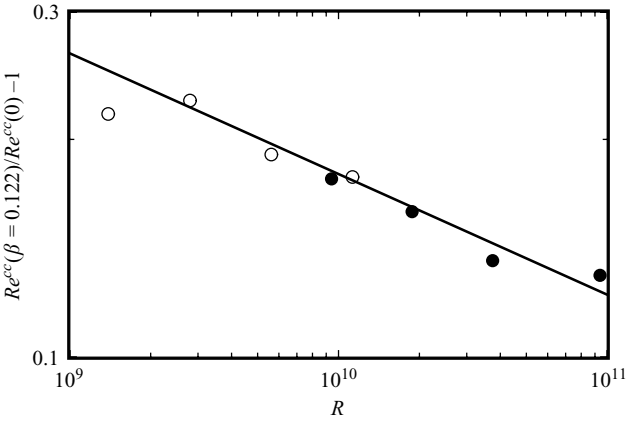

FIGURE 18. The Reynolds-number ratio $Re^{cc}(\beta = 0.122)/Re^{cc}(0)$ of the LSC as a function of R. Open circles: medium sample. Solid circles: large sample. Solid line: power law with an exponent of 1/6.

The Rayleigh-number dependence of Re^{cc} at constant β is shown in figure 18. Here the open (solid) circles are from the medium (small) sample. There is consistency between the two samples, and the data can be described by a power law with a small negative exponent. The solid line is drawn to correspond to an exponent of $-1/6$.

5.4. *A model for the enhancement of the Reynolds number*

As seen in figure 10, the LSC assumes an orientation for which gravity enhances the velocity above (below) the bottom (top plate), i.e. the LSC flows 'uphill' at the bottom where it is relatively warm and 'downhill' at the top where it is relatively cold. This leads to an enhancement of the Reynolds number of the LSC. As suggested by Chillà *et al.* (2004), one can model this effect by considering the buoyancy force per unit area parallel to the plates. This force can be estimated to be $\rho l g \beta \alpha \Delta T/2$ where l is the boundary-layer thickness. It is opposed by the increase of the viscous shear stress across the boundary layer that may be represented by $\rho \nu u'/l$ where u' is the extra

speed gained by the LSC due to the tilt. Equating the two, substituting

$$l = L/(2\mathscr{N}), \tag{5.8}$$

solving for u', using (1.2) for R, and defining $Re' \equiv (L/\nu)u'$ one obtains

$$Re' = \frac{R\beta}{8\sigma\mathscr{N}^2} \tag{5.9}$$

for the enhancement of the Reynolds number of the LSC. From our measurements at large R we found that Re and $\mathscr{N}$ (Nikolaenko *et al.* 2005) can be represented within experimental uncertainty by

$$Re = 0.0345R^{1/2}, \tag{5.10}$$

$$\mathscr{N} = 0.0602R^{1/3}, \tag{5.11}$$

giving

$$\frac{Re'}{Re} = 1.00 \times 10^3 R^{-1/6}\sigma^{-1}\beta. \tag{5.12}$$

For our $\sigma = 4.38$ and $R = 9.43 \times 10^{10}$ one finds $Re'/Re = 3.4\beta$, compared to the experimental value $(1.9 \pm 0.2)\beta$ from Re^{cc} (equation (5.6)) and $(1.7 \pm 0.4)\beta$ from Re^{ac} (equation (5.7)). We note that the coefficient 1.00×10^3 in (5.12) depends on the definition of Re given in (5.4) and (5.5) that was used in deriving the result (5.10). If the length scale $4L$ had been used instead of $2L$ to define the speed of the LSC, as was done for instance by Lam *et al.* (2002), this coefficient would have been smaller by a factor of two, yielding near-perfect agreement with the measurements. In figure 18 the predicted dependence on $R^{-1/6}$ also is in excellent agreement with the experimental results. However, such good agreement may be somewhat fortuitous, considering the approximations that were made in the model. Particularly the use of (5.8) for the boundary-layer thickness is called into question at a quantitative level by measurements of Lui & Xia (1998) that revealed a significant variation of l with lateral position. In addition, it is not obvious that the thermal boundary-layer thickness l should be used, as suggested by Chillà *et al.* (2004), to estimate the shear stress; perhaps the thickness of the viscous boundary layer would be more appropriate.

In discussing their $\Gamma = 0.5$ sample, Chillà *et al.* (2004) took the additional step of assuming that the relative change of $\mathscr{N}$ due to a finite β is equal to the relative change of Re. For our sample with $\Gamma = 1$ this assumption does not hold. As we saw above, the relative change of $\mathscr{N}$ is a factor of about 50 less than the relative change of Re. The origin of the (small) reduction of the Nusselt number is not obvious. Naively one might replace g in the definition of the Rayleigh number by $g\cos(\beta)$; but this would lead to a correction of order β^2 whereas the experiment shows that the correction is of order β, albeit with a coefficient that is smaller than of order one. The linear dependence suggests that the effect of β on $\mathscr{N}$ may be provoked by the change of Re with β, but not in a direct causal relationship.

6. Tilt-angle dependence of reorientations of the large-scale circulation

It is known from direct numerical simulation (Hansen, Yuen & Kroening 1991) and from several experiments (Cioni, Ciliberto & Sommeria 1997; Niemela *et al.* 2001; Sreenivasan *et al.* 2002; Brown *et al.* 2005*a*) that the LSC can undergo relatively sudden reorientations. Not unexpectedly, we find that the tilt angle strongly influences the frequency of such events. For a level sample ($\beta = 0$) we demonstrated elsewhere (Brown *et al.* 2005*a*) that reorientations can involve changes of the orientation of the

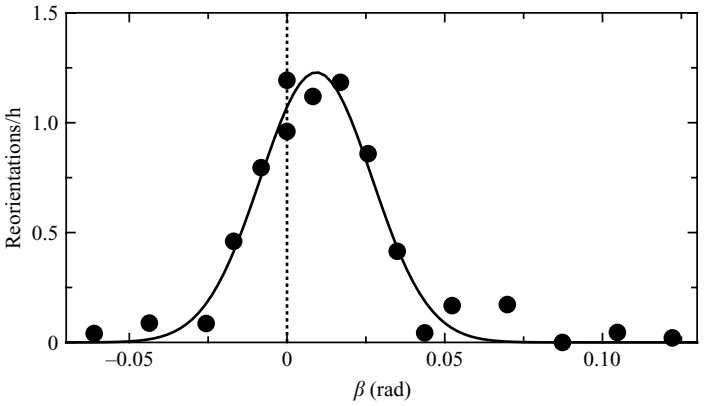

FIGURE 19. The number of reorientation events per hour of the angular orientation of the plane of circulation of the LSC in the large sample for $R = 9.43 \times 10^{10}$. The solid line shows (6.1).

plane of circulation of the LSC through any angular increment $\Delta\theta$, with the probability $P(\Delta\theta)$ increasing with decreasing $\Delta\theta$. Thus, in order to define a 'reorientation', we established certain criteria. We required that the magnitude of the net angular change $|\Delta\theta|$ had to be greater than $\Delta\theta_{min} = (2\pi)/8$. In addition we specified that the magnitude of the net average azimuthal rotation rate $|\dot{\theta}| \equiv |\Delta\theta/\Delta t|$ had to be greater than $\dot{\theta}_{min} = 0.1/\mathscr{T}$ where $\mathscr{T}$ is the LSC turnover time and Δt is the duration of the reorientation (we refer to Brown *et al.* (2005*a*) for further details). Using these criteria, we found that the number of reorientation events $n(\beta)$ at constant $R = 9.43 \times 10^{10}$ decreased rapidly with increasing $|\beta|$. These results are shown in figure 19. It is worth noting that nearly all of these events are rotations of the LSC and very few involved a cessation of the circulation. A least-squares fit of the Gaussian function

$$n(\beta) = N_0 \exp[-(\beta - \beta_0)^2/w^2] \tag{6.1}$$

to the data yielded $N_0 = 1.23 \pm 0.06$ events per hour, $\beta_0 = 0.0093 \pm 0.0010$ rad, and $w = 0.0251 \pm 0.0015$ rad. It is shown by the solid line in the figure.

We note that the distribution function is not centred on $\beta = 0$. The displacement of the centre by about 9 mrad is much more than the probable error of β. We believe that it is caused by the effect of the Coriolis force on the LSC that will be discussed in more detail elsewhere (Brown & Ahlers 2006).

7. Tilt-angle dependence of the centre temperature

We saw from figure 13 that the increase of Re with β led to an increase of the amplitude δ of the azimuthal temperature variation at the horizontal mid-plane. An additional question is whether the tilt-angle effect on this system has an asymmetry between the top and bottom that would lead to a change of the mean centre temperature T_c (see (2.1)). Chillà *et al.* (2004) report such an effect for their $\Gamma = 0.5$ sample. For a Boussinesq sample with $\beta = 0$ we expect that $T_c = T_m$ with $T_m = (T_t + T_b)/2$ (T_t and T_b are the top and bottom temperatures respectively), or equivalently that $\Delta_t = T_c - T_t$ is equal to $\Delta_b = T_b - T_c$. A difference between Δ_b and Δ_t will occur when the fluid properties have a significant temperature dependence (Wu & Libchaber 1991; Zhang, Childress & Libchaber 1997; Ahlers *et al.* 2006), i.e. when there are significant deviations from the Boussinesq approximation. For the sequence of measurements with the large apparatus and $R = 9.43 \times 10^{10}$, as a function of β the

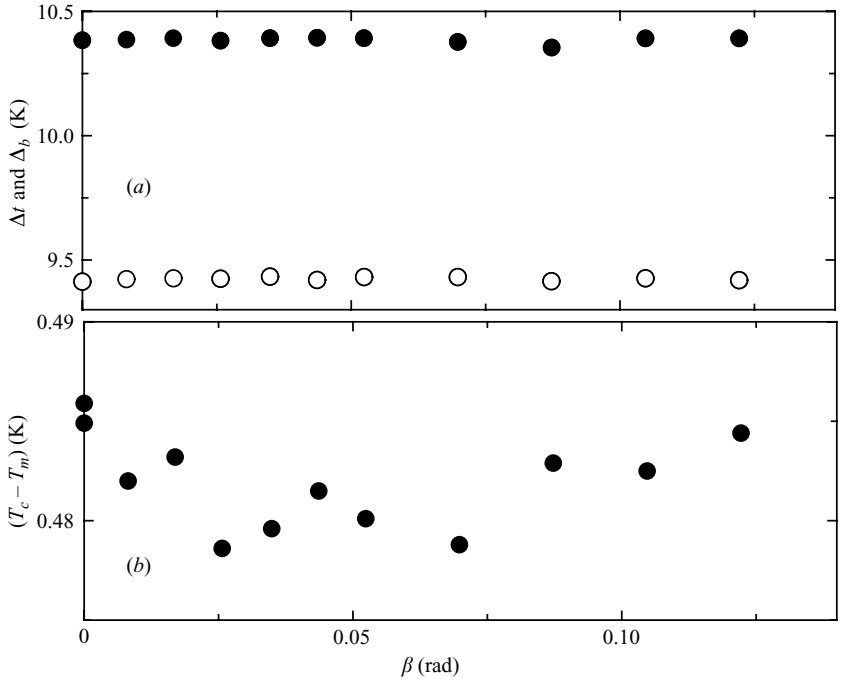

FIGURE 20. (*a*) The temperature difference in Kelvin between the bottom and the centre ($\Delta_b = T_b - T_c$, solid circles) and the centre and the top ($\Delta_t = T_c - T_t$, open circles) as a function of the tilt angle β. (*b*) The temperature difference $T_c - T_m = (\Delta_t - \Delta_b)/2$ between the centre temperature T_c and the mean temperature $T_m = (T_t + T_b)/2$. The centre temperature is the average of the values given by the eight sidewall thermometers.

mean value of $\Delta T = T_b - T_t$ was 19.808 ± 0.018°C and $T_c - T_m$ was 0.485°C, indicating a significant non-Boussinesq effect. In figure 20(*a*) we show Δ_t and Δ_b as a function of β. Increasing β does not have a significant effect for our $\Gamma = 1$ sample. This is shown with greater resolution in figure 20(*b*) where $T_c - T_m = (\Delta_t - \Delta_b)/2$ is shown. We believe that the small variation, over a range of about 5×10^{-3}°C, is within possible systematic experimental errors and consistent with the absence of a tilt-angle effect.

8. Summary

In this paper we report on an experimental investigation of the influence on turbulent convection of a small tilt angle β relative to gravity of the axes of two cylindrical Rayleigh–Bénard samples. The aspect ratios were $\Gamma \simeq 1$.

Where there was overlap, there were significant differences between our results and those obtained by Chillà *et al.* (2004) for a $\Gamma = 0.5$ sample. Presumably these differences are attributable to the different LSC structures for $\Gamma = 1$ and $\Gamma = 0.5$. We found our system to establish a statistically stationary state quickly, within a couple of hours, after a Rayleigh-number change whereas Chillà *et al.* (2004) found long transients that they attributed to changes of the LSC structure. We found a very small reduction of the Nusselt number $\mathcal{N}$ with increasing β, by about 4 % per radian at small β. Chillà *et al.* (2004) found a decrease by 200 % per radian for their sample.

In contrast to the very small effect of β on $\mathcal{N}$, we found an increase of the Reynolds number Re by about 180 % per radian for small β. The small effect on $\mathcal{N}$ in the presence of this large change of Re indicates that the heat transport does not depend

strongly on the speed of the LSC sweeping over the boundary layers. Instead, $\mathscr{N}$ must be determined by instability mechanisms of the boundary layers, and the associated efficiency of the ejection of hot (cold) volumes (so-called 'plumes') of fluid from the bottom (top) boundary layer.

It is interesting to note that the strong dependence of Re on β in the presence of only a very weak dependence of $\mathscr{N}$ on β can be accommodated quite well within the model of Grossmann & Lohse (2002). The Reynolds number can be changed by introducing a β-dependence of the parameter $a(\beta)$ in their equations (4) and (6). As pointed out by them, a change of a has no influence on the predicted value for $\mathscr{N}$.

We also measured the frequency of rapid LSC reorientations that are known to occur for $\beta = 0$. We found that such events are strongly suppressed by a finite β. Even a mild breaking of the rotational invariance, corresponding to $\beta \simeq 0.04$, suppresses re-orientations almost completely.

We are grateful to Siegfried Grossmann and Detlef Lohse for fruitful exchanges. This work was supported by the United States Department of Energy through Grant DE-FG02-03ER46080.

REFERENCES

Ahlers, G., Brown, E., Fontenele Araujo, F., Funfschilling, D., Grossmann, S. & Lohse, D. 2006 Non-Oberbeck-Boussinesq effects in strongly turbulent Rayleigh–Bénard convection. *J. Fluid Mech.*, submitted.

Ahlers, G., Grossmann, S. & Lohse, D. 2002 Hochpräzision im Kochtopf: Neues zur turbulenten Konvektion. *Physik J.* **1**(2), 31–37.

Belmonte, A., Tilgner, A. & Libchaber, A. 1995 Turbulence and internal waves in side-heated convection. *Phys. Rev.* E **51**, 5681–5687.

Brown, E. & Ahlers, G. 2006 Effect of Earth's Coriolis force on the large-scale circulation in turbulent Rayleigh-Bénard convection in the laboratory. *J. Fluid Mech.* (submitted)

Brown, E., Nikolaenko, A. & Ahlers, G. 2005*a* Orientation changes of the large-scale circulation in turbulent Rayleigh-Bénard convection. *Phys. Rev. Lett.* **95**, 084503-1–4.

Brown, E., Nikolaenko, A., Funfschilling, D. & Ahlers, G. 2005*b* Heat transport in turbulent Rayleigh–Bénard convection: Effect of finite top- and bottom-plate conductivity. *Phys. Fluids* **17**, 075108.

Castaing, B., G. Gunaratne, G., Heslot, F., Kadanoff, L., Libchaber, L., Thomae, S., Wu, X.-Z., Zaleski, S. & Zanetti, G. 1989 Scaling of hard thermal turbulence in Rayleigh–Bénard convection. *J. Fluid Mech.* **204**, 1–30.

Chaumat, S., Castaing, B. & Chillà, F. 2002 Rayleigh–Bénard cells: influence of the plates properties *Advances in Turbulence IX, Proc. Ninth European Turbulence Conf.* (ed. I. P. Castro & P. E. Hancock). CIMNE, Barcelona.

Chillà, F., Rastello, M., Chaumat, S. & Castaing, B. 2004 Long relaxation times and tilt sensitivity in Rayleigh–Bénard turbulence. *Eur. Phys. J.* B **40**, 223–227.

Ciliberto, S., Cioni, S. & Laroche, C. 1996 Large-scale flow properties of turbulent thermal convection. *Phys. Rev.* E **54**, R5901–R5904.

Cioni, S., Ciliberto, S. & Sommeria, J. 1997 Strongly turblent Rayleigh–Bénard convection in mercury: comparison with results at moderate Prandtl number. *J. Fluid Mech.* **335**, 111–140.

Funfschilling, D., Brown, E., Nikolaenko, A. & Ahlers, G. 2005 Heat transport by turbulent Rayleigh–Bénard Convection in cylindrical samples with aspect ratio one and larger. *J. Fluid Mech.* **536**, 145–154.

Grossmann, S. & Lohse, D. 2001 Thermal convection for large Prandtl number. *Phys. Rev. Lett.* **86**, 3317–3319.

Grossmann, S. & Lohse, D. 2002 Prandtl and Rayleigh number dependence of the Reynolds number in turbulent thermal convection. *Phys. Rev.* E **66**, 016305, 1–6.

Hansen, U., Yuen, D. A. & Kroening, S. E. 1991 Mass and heat transport in strongly time-dependent thermal convection at infinite Prandtl number. *Geophys. Astrophys. Fluid Dyn.* **63**, 67–89.

Kadanoff, L. P. 2001 Turbulent heat flow: Structures and scaling. *Phys. Today* **54** (8), 34–39.

Kraichnan, R. 1962 Turbulent thermal convection at arbitrary Prandtl number. *Phys. Fluids* **5**, 1374–1389.

Krishnamurty, R. & Howard, L. N. 1981 Large-scale flow generation in turbulent convection. *Proc. Natl Acad. Sci. USA* **78**, 1981–1985.

Lam, S., Shang, X.-D. & Xia, K.-Q. 2002 Prandtl number dependence of the viscous boundary layer and the Reynolds numbers in Rayleigh–Bénard convection. *Phys. Rev.* E **65**, 066306 1–8.

Lui, S.-L. & Xia, K.-Q.1998 Spatial structure of the thermal boundary layer in turbulent convection. *Phys. Rev.* E **57**, 5494–5503.

Niemela, J., Skrbek, L., Sreenivasan, K. & Donnelly, R. 2001 The wind in confined thermal Convection. *J. Fluid Mech.* **449**, 169–178.

Nikolaenko, A., Brown, E., Funfschilling, D. & Ahlers, G. 2005 Heat transport by turbulent Rayleigh–Bénard Convection in cylindrical cells with aspect ratio one and less. *J. Fluid Mech.* **523**, 251–260.

Qiu, X.-L. & Tong, P. 2001*a* Large-scale velocity structures in turbulent thermal convection. *Phys. Rev.* E **64**, 036304, 1–13.

Qiu, X.-L. & Tong, P. 2001*b* Onset of coherent oscillations in turbulent Rayleigh–Bénard convection. *Phys. Rev. Lett.* **87**, 094501, 1–4.

Qiu, X.-L. & Tong, P. 2002 Temperature oscillations in turbulent Rayleigh–Bénard convection. *Phys. Rev.* E **66**, 026208, 1–11.

Roche, P.-E., Castaing, B., Chabaud, B. & Hébral, B. 2004 Heat transfer in turbulent Rayleigh–Bénard convection below the ultimate regime. *J. Low Temp. Phys.* **134**, 1011–1042.

Shraiman, B. I. & Siggia, E. D. 1990 Heat transport in high-Rayleigh number convection. *Phys. Rev.* A **42**, 3650–3653.

Siggia, E. D. 1994 High Rayleigh number convection. *Annu. Rev. Fluid Mech.* **26**, 137–168.

Sreenivasan, K., Bershadskii, A. & Niemela, J. 2002 Mean wind and its reversal in thermal convection. *Phys. Rev.* E **65**, 056306, 1–11.

Stringano, G. & Verzicco, R. 2006 Mean flow structure in thermal convection in a cylindrical cell of aspect-ratio one half. *J. Fluid Mech.* **548**, 1–16.

Sun, C., Xi, H.-D. & Xia, K.-Q. 2005*a* Azimuthal symmetry, flow dynamics, and heat flux in turbulent thermal convection in a cylinder with aspect ratio one-half. *Phys. Rev. Lett* **95**, 074502-1–4.

Sun, C., Xia, K.-Q. & Tong, P. 2005*b* Three-dimensional flow structures and dynamics of turbulent thermal convection in a cylindrical cell. *Phys. Rev.* E **72**, 026302, 1–13.

Verzicco, R. 2004 Effects of non-perfect thermal sources in turbulent thermal convection. *Phys. Fluids* **16**, 1965–1979.

Verzicco, R. & Camussi, R. 2003 Numerical experiments on strongly turbulent thermal convection in a slender cylindrical cell. *J. Fluid Mech.* **477**, 19–49.

Wu, X.-Z. & Libchaber, A. 1991 Non-Boussinesq effects in free thermal convection. *Phys. Rev.* A **43**, 2833–2839.

Xi, H.-D., Lam, S. & Xia, K.-Q. 2004 From laminar plumes to organized flows: the onset of large-scale circulation in turbulent thermal convection. *J. Fluid Mech.* **503**, 47–56.

Zhang, J., Childress, S. & Libchaber, A. 1997 Non-Boussinesq effect: Thermal convection with broken symmetry. *Phys. Fluids* **9**, 1034–1042.